Dendritic glutamate release produces autocrine activation of mGluR1 in cerebellar Purkinje cells

Jung Hoon Shin, Yu Shin Kim, and David J. Linden*

Department of Neuroscience, The Johns Hopkins University School of Medicine, 725 North Wolfe Street, 916 Hunterian Building, Baltimore, MD 21205

In recent years, it has become clear that, in addition to conventional anterograde transmission, signaling in neural circuits can occur in a retrograde manner. This suggests the additional possibility that postsynaptic release of neurotransmitter might be able to act in an autocrine fashion. Here, we show that brief depolarization of a cerebellar Purkinje cell triggers a slow inward current. This depolarization-induced slow current (DISC) is attenuated by antagonists of mGluR1 or TRP channels. DISC is eliminated by a mixture of voltage-sensitive Ca^{2+} channel blockers and is mimicked by a brief climbing fiber burst. DISC is attenuated by an inhibitor of vesicular glutamate transporters or of vesicular fusion. These data suggest that Ca^{2+}-dependent postsynaptic fusion of glutamate-loaded vesicles evokes a slow inward current produced by activation of postsynaptic mGluR1, thereby constituting a useful form of feedback regulation.

Ca channel | retrograde signaling | vesicular fusion

Retrograde signaling in neural circuits is often triggered by a postsynaptic Ca^{2+} flux driven by activity. This can evoke the release of two broad classes of signal: those triggered by Ca^{2+}-sensitive enzymatic synthesis, like NO and endocannabinoids (although in some cases, endocannabinoid synthesis is Ca^{2+}-independent), and those that require postsynaptic vesicular fusion, like classical neurotransmitters and peptide hormones. In the olfactory bulb, it is well established that action potential invasion of mitral cell dendrites triggers dendritic glutamate release, which then excites the dendrites of adjacent granule cells (1). In other brain regions, such as neocortical layer 2/3 pyramidal cells, the postsynaptic release of glutamate has been inferred from experiments in which postsynaptic depolarization triggers a depression of inhibitory postsynaptic potentials (IPSPs) or inhibitory postsynaptic currents (IPSCs) evoked by activation of fast-spiking interneurons. In these experiments, this effect was blocked by postsynaptic Ca^{2+} chelation, manipulations to interfere with the loading or fusion of postsynaptic glutamate-containing vesicles, or blockade of group II mGluRs (presumably located on the interneuron terminals), but not by antagonists of CB1 receptors (2, 3).

Cerebellar Purkinje cells release GABA from axonal terminals, but it has been suggested they may also release glutamate from their dendrites and/or soma (4). Brief depolarization of Purkinje cells triggered a persistent increase in the frequency of mIPSCs, a phenomenon termed depolarization-induced potentiation of inhibition (DPI). DPI was blocked by postsynaptic Ca^{2+} chelation or treatments that blocked SNARE-dependent vesicular fusion (Botulinum toxin B, GDPbetaS). In addition, bath application of an NMDA receptor antagonist but not a CB1 receptor antagonist blocked DPI. It was proposed that Ca^{2+}-triggered fusion of vesicles in Purkinje cell dendrites released glutamate, which then diffused to activate NMDA receptors on interneuron terminals (4, 5). If this model is correct, then glutamate released from dendrites may also have access to glutamate receptors in those same dendrites, allowing for recurrent self-excitation, an autocrine effect.

Results

Whole-cell voltage−clamp recordings were made from Purkinje cells in cerebellar slices derived from postnatal day 15–18 (P15–18) rats. A test stimulus, consisting of five 10-msec-long depolarizing command pulses from −70 to 0 mV at 10 Hz, was delivered with an interstimulus interval of 30 s. GABAzine (5 μM) was added to the external saline to block $GABA_A$ receptors. The depolarizing stimulus evoked a biphasic inward current recorded at a holding potential of −70 mV (Fig. 1a). The earlier portion of the inward current (Fig. 1a, open circle) reversed near the predicted E_{Cl} of −66.2 mV (Fig. 1b) and is likely to be mediated, at least in large part, by a Ca^{2+}-dependent Cl^- conductance, as described (6). In our hands, this early portion of the inward current was quite variable and labile. However, the later portion of the inward current (Fig. 1a, filled circle) typically reached a stable amplitude ≈20 min after the establishment of whole-cell recording and could be recorded in a stable fashion for an additional 20–40 min (Fig. 1c). We have called this later component depolarization-induced slow current (DISC). DISC had a time to peak of 1.80 ± 0.12 sec, a peak amplitude of 509.20 ± 40.04 pA, and a 90–10% decay time of 2.81 ± 0.30 sec (mean ± SEM; $n = 26$).

DISC was associated with a significant increase in the current noise above baseline values (Fig. 2a). This property has been reported for an mGluR1-mediated slow inward current recorded in Purkinje cells in response to exogenous mGluR1 agonist or burst stimulation of glutamatergic parallel fibers (7, 8). In addition to mGluR1, Purkinje cells express AMPA and kainate receptors but not functional NMDA receptors. When the AMPA/kainate receptor antagonist 2,3-dihydroxy-6-nitro-7-sulfamoylbenzo[f]quinoxaline (NBQX) was bath-applied at a concentration of 100 μM, DISC was not significantly attenuated compared with the untreated group ($P = 0.410$; Fig. 2b). The ratio of DISC charge transfer measured 10 min after NBQX application to the pre-NBQX time point was 0.92 ± 0.03 (mean ± SEM; $n = 5$). For a saline control group measured at the same time point, this ratio was 0.97 ± 0.05 ($n = 5$). Bath application of the mGluR1α antagonist CPCCOEt (100 μM) produced a significant but not total blockade of DISC (0.29 ± 0.06, $n = 5$, $P = 0.001$ compared with control; Fig. 2c). A similar effect was seen by using a different mGluR1 antagonist, JNJ 16259685 (50 μM; 0.23 ± 0.07, $n = 5$, $P < 0.001$ compared with control; Fig. 2d), as well as a somewhat less-specific drug, the mGluR1/5 antagonist (R,S)-1-aminoindan-1,5-dicarboxylic acid (AIDA, 100 μM; data not shown). The mGluR1-mediated inward current in Purkinje cells is carried by cation conductance

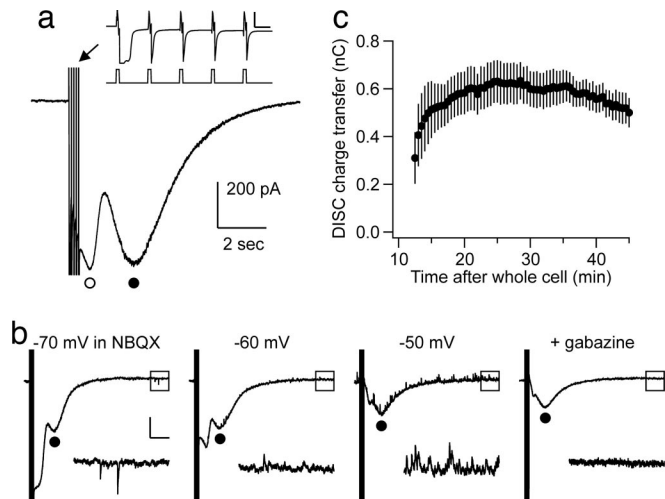© 2008 by The National Academy of Sciences of the USA

Fig. 1. Purkinje cell depolarization induces a biphasic inward current with fast and slow components. (*a*) A train of depolarizing command pulses from −70 to 0 mV was given, as illustrated in *Inset*. This train consisted of five pulses, each 10 msec long, with an interpulse interval of 100 msec. (*Inset* calibration bars: 2 nA, 50 msec.) This induced a biphasic inward current with fast (open circle) and slow (filled circle) components. (*b*) Depolarizing command pulses were given from different holding voltages, and the resultant inward currents were measured. The slow component was marked with filled circles. In these recordings, 20 μM NBQX was added, and a GABA$_A$ receptor antagonist was omitted to allow for simultaneous recording of spontaneous IPSCs and comparison of their reversal with that of both components of the biphasic inward current. Lower traces are expanded from the squares. E_{Cl} was calculated to be −66.2 mV. (Calibration bars: 200 pA, 2 sec.) (*c*) We call the slow component of this response ''depolarization induced slow current'' (DISC). In this graph, DISC charge transfer was measured, and the mean ± SE was plotted as a function of time (*n* = 5).

that requires the ion channel TrpC1 (9). Specific antagonists of TrpC1 are not available, but SKF 96365 is a nonspecific drug that will block TrpC1 as well as other ion channels. Bath application of SKF 96365 (30 μM) produced an attenuation of DISC that was similar to that produced by mGluR1 antagonists (0.36 ± 0.09, *n* = 5, *P* = 0.003 compared with control; Fig. 2*e*). CPCCOEt (100 μM), JNJ 16259685 (50 μM), and SKF 96365 (30 μM) all produced a significant attenuation of the increase in current noise associated with DISC (0.30 ± 0.06, *n* = 5, *P* < 0.001; 0.29 ± 0.10, *n* = 5, *P* < 0.001; and 0.54 ± 0.12, *n* = 5, *P* = 0.004, respectively). Furthermore, DISC was not significantly attenuated when TTX was added (500 nM; *n* = 3), or when the slice was presoaked in an NMDA-R antagonist, (*R*)-CPP (20 μM; *n* = 5) [supporting information (SI) Fig. 5 *b* and *c*].

If depolarization of Purkinje cell dendrites triggers vesicular fusion, this process is likely to require Ca^{2+} influx (SI Fig. 6). As a test of this idea, we applied a mixture of specific Ca^{2+} channel blockers, the P/Q blocker ω-agatoxin IVA (0.2 μM), the N blocker ω-conotoxin MVIIC (3 μM), and the L blocker nifedipine (3 μM). This produced a complete blockade of DISC charge transfer and the DISC-associated increase in current noise (−0.01 ± 0.01 and −0.05 ± 0.02, respectively; *n* = 5; *P* < 0.001 compared with control; Fig. 2*f*). Similar results were obtained when Cd^{2+} (250 μM) was applied (0.00 ± 0.00 and −0.01 ± 0.02, respectively; *n* = 5; *P* < 0.001 compared with control; Fig. 2*g*). It is worthwhile to note that mGluR1-mediated current in Purkinje cells is blocked by strong Ca^{2+} chelation (10), so it is not possible to perform an experiment in which DISC blockade is measured in Purkinje cells loaded with a high concentration of Ca^{2+} chelator.

The loading of glutamate into vesicles presumably requires the operation of a vesicular glutamate transporter that is driven by
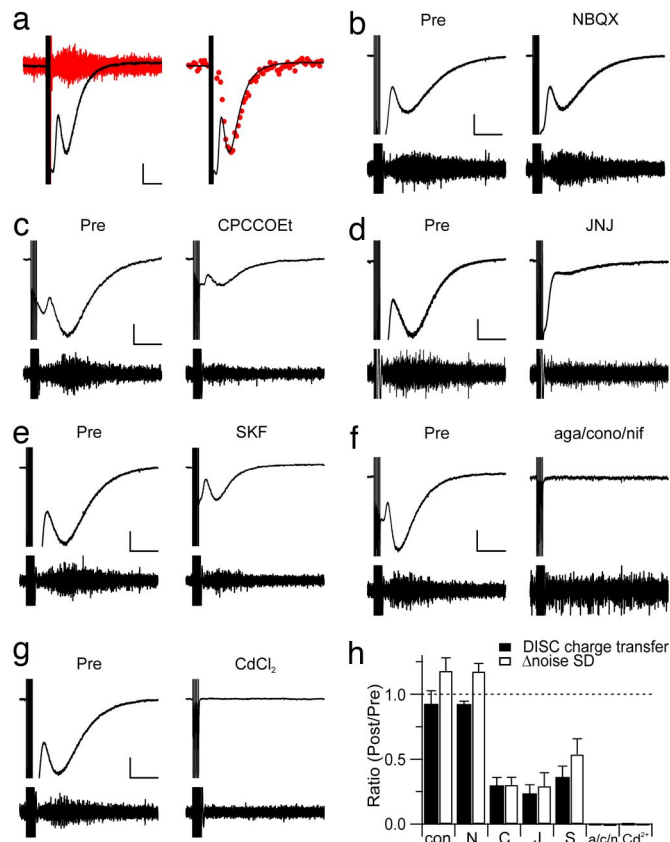

Fig. 2. DISC is Ca^{2+}-triggered and involves activation of mGluR1 and TrpC1 cation channels. (*a Left*) When single-exemplar current traces were high-pass-filtered at 10 Hz, this revealed a significant increase in noise at the peak of DISC (red). [Calibration bars: 100 pA, 2 sec (current trace); 10 pA, 0.2 sec (filtered trace).] (*Right*) The standard deviation was calculated from 200-msec-long segments of the high-pass-filtered traces to yield the noise SD. Noise SD values from five sequential episodes (red circles) were scaled and superimposed on the current trace, which is an average of the same five episodes. (*b–g*) Both current and the high-pass-filtered traces were plotted before and after application of various receptor antagonists or channel blockers (100 μM NBQX; 100 μM CPCCOEt; 50 μM JNJ 16259685; 30 μM SKF 96365; a mixture of 0.2 μM ω-agatoxin IVA, 3 μM ω-conotoxin MVIIC, and 3 μM nifedipine; or 250 μM Cd^{2+}). [Calibration bars: 200 pA, 2 sec (current traces).] The high-pass-filtered traces are displayed by using a range of −25 to 25 pA. (*h*) The averages of either DISC charge transfer (filled bars) or Δ noise SD (open bars) are plotted as a ratio of measurements 20 min after drug application to a preexposure baseline (con, control; N, NBQX; C, CPCCOEt; J, JNJ 16259685; S, SKF96365; a/c/n: mixture of Ca^{2+} channel blockers).

a H$^+$ gradient. This gradient is established by the operation of a vacuolar-type H$^+$-ATPase. We added bafilomycin A1 (500 nM), an inhibitor of vacuolar-type H$^+$-ATPase, to the internal saline and then compared DISC at an early time point (when DISC charge transfer is typically stable in recordings with normal internal saline) with DISC at a later time point when the drug has more completely perfused the extensive Purkinje cell dendrite (Fig. 3*a*, upper trace; Fig. 3*c*). The ratio of DISC charge transfer at 40 min to that at 20 min after achieving the whole-cell configuration was used as an index of drug action. Bafilomycin A1 perfusion yielded a ratio of 0.35 ± 0.07 (*n* = 4, *P* < 0.001 compared with carrier solution), whereas a DMSO carrier solution control produced a ratio of 1.17 ± 0.08 (*n* = 5). As a control, the peak amplitude of the inward current induced by puffing an mGluR1 agonist, 3,5-dihydroxyphenylglycine (DHPG) (150 μM) in molecular layer was measured. These responses were not attenuated by internal perfusion with bafilo-
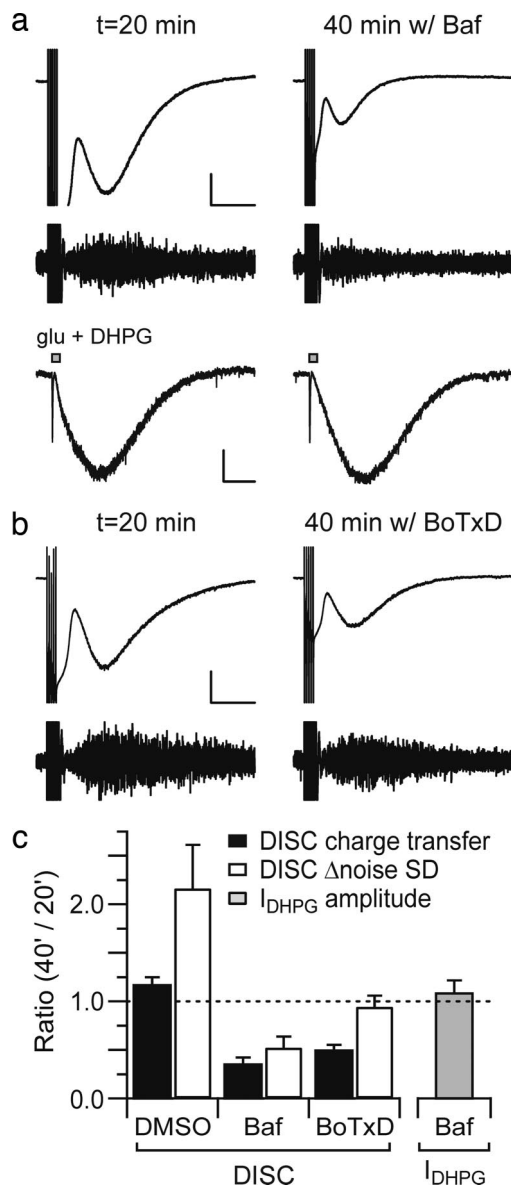
Fig. 3. Internal application of blockers of either vacuolar H$^+$-ATPase or SNARE-dependent vesicular fusion suppresses DISC. Either bafilomycin A1 (500 nM) (*a*) or BoTxD (100 nM) (*b*) was added to the internal saline. [Calibration bar: 300 pA, 2 sec (current trace).] The high-pass-filtered traces are displayed by using a range of −25 to 25 pA (*a Lower*). For control experiments to address side effects on mGluR1/TrpC1 signaling, an mGluR1 agonist, DHPG (150 μM), together with glutamate (10 μM), was pressure-ejected (10 psi, 50 msec) in the inner one-third of the molecular layer to induce both fast (AMPA/kainate receptor-mediated) and slow (mGluR1-mediated) inward currents. Slow currents (I_{DHPG}) are measured in cells perfused with bafilomycin A1. (Calibration bar: 100 pA, 2 sec.) (*c*) The average ratios of DISC charge transfer (filled), Δ noise SD (open), or I_{DHPG} amplitude (gray) are plotted. The ratio reflects the value at $t = 40$ min/$t = 20$ min.

mycin A1-containing solution (1.08 ± 0.13, $n = 5$; Fig. 3*a*, lower trace; Fig. 3*c*). This argues that bafilomycin A1 is attenuating DISC through an action on vacuolar-type H$^+$-ATPase rather than through a side effect on the mGluR1 signaling cascade. A similar internal perfusion approach was taken to deliver Botulinum toxin D (BoTxD; 100 nM), an inhibitor of SNARE-mediated vesicular fusion by cleaving synaptobrevin, to the Purkinje cell dendrite. BoTxD produced a DISC attenuation ratio of 0.49 ± 0.06 ($n = 5$, $P = 0.007$ compared with control;

Fig. 3 *b* and *c*). It should be cautioned that this design is likely to underestimate the effects of internally applied drugs. First, it is likely that some drug has reached the target sites in the dendrite before $t = 20$ min. Second, it is possible that saturating concentrations of drug have not been achieved at all target sites (including the most distal portion of the dendrite) at $t = 40$ min. Importantly, none of drugs used herein to block DISC (SKF 96365, BoTxD, CPCCOEt, JNJ 16259685, and bafilomycin A1) had side effects on depolarization-evoked dendritic Ca^{2+} transients, as measured by using laser-scanning confocal microscopy (SI Fig. 7).

The size of DISC was not significantly different from the control group when Purkinje cells were loaded with a solution that contained 135 mM L-glutamate (486.79 ± 68.58 pA, $n = 11$; SI Fig. 5*d*). Perhaps the concentration of cytosolic glutamate is not limiting for the filling of the vesicles. Alternatively, it is possible that high internal glutamate has some unforeseen side effects.

Is it possible there is a component of postsynaptic glutamate release underlying DISC that is independent of vesicular fusion? One candidate mechanism is reverse operation of EAAT3 and EAAT4 glutamate transporters in the Purkinje cell plasma membrane. To test this hypothesis, DISC was measured in brain slices derived from EAAT3/EAAT4 double-knockout mice and was found to be unimpaired (1,051 ± 73 pA, $n = 8$) compared with wild-type mice (860 ± 90 pA, $n = 8$; SI Fig. 8).

Depolarization of Purkinje cells causes endocannabinoid release. One candidate endocannabinoid is anandamide, which has been shown to be a TRP channel agonist (11). When we applied an inhibitor of anandamide (fatty acid amide) hydrolase, URB597 (5 μM), the size of DISC was not increased but rather was slightly attenuated (0.76 ± 0.07, $n = 5$). Furthermore, exogenous puff application of anandamide in the presence of URB597 failed to evoke an inward current or an increase in the noise SD (data not shown). These results argue against a role for anandamide in triggering DISC.

DISC could also be evoked by physiologically relevant climbing fiber-burst stimulation. Noxious pinch can cause climbing fiber firing at up to 11 Hz for the duration of the stimulus, lasting several seconds (12). In fact, these experiments were performed in pentobartitone-anesthetized cats and are therefore likely to underestimate the rate of pinch-evoked climbing fiber firing. In the present experiments, Cs$^+$-loaded Purkinje cells were stimulated by brief climbing fiber bursts (five pulses at 10 Hz) in voltage–clamp mode with a command potential of −55 mV (Fig. 4*a*). Immediately after termination of the burst, a slow inward current (CF-DISC) was recorded. This CF-DISC has a time to peak (1.45 ± 0.29 sec) and noise envelope similar to DISC evoked by somatic depolarization. CF-DISC is completely blocked by 0.5 μM NBQX (this concentration decreased the climbing fiber EPSC to 16.4 ± 1.6% of control, $n = 5$) consistent with a requirement for CF-driven depolarization (clamp failure during the bursts). An mGluR1 antagonist, CPCCOEt (100 μM), decreased the CF-DISC charge transfer and Δnoise SD to 34.2 ± 6.4% and 35.4 ± 7.4% of control, respectively ($n = 5$; Fig. 4 *b* and *c*).

Discussion

The results herein suggest the following model. Depolarization of Purkinje cell dendrites triggers Ca^{2+} influx through voltage-sensitive Ca^{2+} channels. The resultant Ca^{2+} elevation activates Ca^{2+}-dependent chloride conductance, underlying the earlier component of the inward current (6), and also triggers SNARE-dependent (BoTxD-sensitive) fusion of vesicles containing glutamate. Glutamate diffuses in the extracellular space and ligates mGluR1 on the same dendrite, producing autocrine activation, which we record as DISC. A caveat that should be noted is the Cs$^+$-based internal solution used herein (to provide adequate
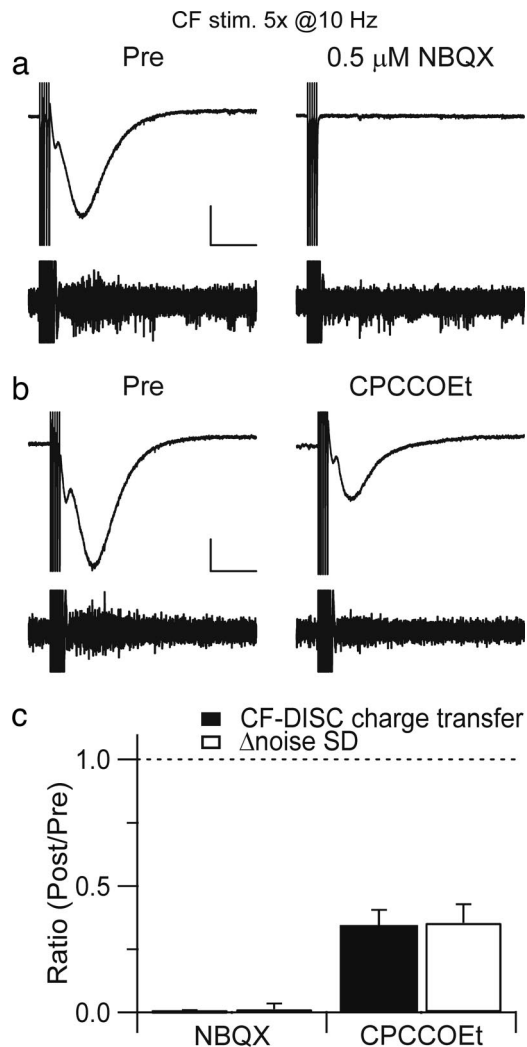
CF stim. 5x @10 Hz

a Pre   0.5 μM NBQX

b Pre   CPCCOEt

c

■ CF-DISC charge transfer
□ Δnoise SD

Ratio (Post/Pre)

NBQX   CPCCOEt

Fig. 4. DISC is evoked by climbing fiber burst stimulation. (*a*) In voltage–clamp mode with a command potential of −55 mV, a climbing fiber was stimulated five times at 10 Hz, which produced a DISC-like inward current (CF-DISC). NBQX (0.5 μM) was subsequently added. (Calibration bar: 300 pA, 2 sec.) (*b*) CPCCOEt was bath-applied at *t* = 20 min. (Calibration bar: 200 pA, 2 sec.) (*c*) The average ratios of CF-DISC charge transfer (filled) and Δ noise SD (open) are plotted. The ratio reflects the value at *t* = 40 min/*t* = 20 min.

voltage–clamp of the extensive Purkinje cell dendrite) will also function to amplify depolarization or climbing fiber burst-evoked Ca^{2+} transients and this amplification may impact the DISC threshold.

The glutamate released during DISC is also likely to diffuse to interneuron terminals, where it activates the NMDA receptors, triggering induction of DPI (4, 5). Although this is the most parsimonious explanation for the present findings, it is also possible that glutamate released from Purkinje cell dendrites could trigger further release of glutamate or some other signaling molecule from another cellular compartment in the cerebellar molecular layer. Cerebellar Bergmann glia express mGluR1 Ca^{2+}-permeable AMPA receptors and P2 receptors and could be a possible source for secondary release of glutamate or ATP. However, Duguid *et al.* (5) have demonstrated DPI in an isolated Purkinje cell soma/inhibitory nerve terminal preparation, arguing against a requirement for glial cells in this process.

The molecular mechanisms underlying postsynaptic release of glutamate have not been carefully examined in any model

system. One candidate molecule for the vesicular glutamate transporter required for DISC is vGluT3, which is reported to be expressed in Purkinje cells (13). The molecular identity of the Ca^{2+} sensor(s) for postsynaptic vesicular fusion and other components of the fusion machinery also await further experiments. We believe DISC will serve as a tractable model system for these investigations.

The present data, together with the findings of Duguid and Smart (4), indicate that glutamate released from Purkinje cells can activate NMDA receptors on interneuron terminals and mGluR1 on the activated Purkinje cell. Glutamate mobility in the extracellular space is controlled by glutamate reuptake into glial cells and, to a lesser extent, glutamate reuptake into Purkinje cell dendrites. It will be interesting to determine whether blockade of glutamate reuptake will be permissive for additional electrophysiological actions such as the activation of glutamate receptors on adjacent Purkinje cells.

In mitral cells of the olfactory bulb, dendritic release of glutamate can produce fast self-excitation through the activation of NMDA and AMPA receptors (14, 15). It should be noted that, unlike the Purkinje cells, mitral cells release glutamate from their axons. Furthermore, they have ultrastructurally typical active zones in their dendrites with docked vesicles, a presynaptic grid, and an opposed postsynaptic density in the granule cell. Thus, it is not completely unexpected that the kinetics of self-excitation in mitral cells is much faster than that reported herein for Purkinje cells (which secrete GABA from their axons and do not have typical active zones in their dendrites).

In hypothalamic neurons, autocrine signaling by the neuropeptides vasopressin and oxytocin occurs on a time scale of minutes (16). In Purkinje cells, self-excitation by DISC is a process with an intermediate time scale (time to peak, ≈1.8 s at room temperature). It is likely that DISC will be induced *in vivo* by climbing fiber excitation, which produces a significant dendritic Ca^{2+} influx. Noxious pinch has been shown to induce sustained climbing fiber bursting at 11 Hz in anesthetized cats (12). It is likely that in unanesthetized animals, higher peak climbing fiber frequencies could be achieved. Climbing fiber activation participates in the induction of several different forms of both short- and long-term synaptic plasticity in Purkinje cells, a number of which require mGluR1 activation, including LTD of parallel fiber-Purkinje cell synapses, suggesting that DISC may participate in these processes.

From a computational perspective, DISC is an interesting event. Its slow time course provides the Purkinje cell with a delayed indicator of strong dendritic activation that may allow it to build timing rules for plasticity that span seconds rather than tens of milliseconds.

Methods

NEUROSCIENCE

−70 to 0 mV at 10 Hz. Pilot studies showed that DISC could also be induced by a single 10-msec-long depolarizing step to 0 mV, but in this case, the DISC response was smaller and more variable. When recorded at 32°C, DISC had a faster time course than at room temperature (SI Fig. 5a) and was more labile. DHPG (150 μM) and glutamate (10 μM) were dissolved in ACSF and pressure-ejected in the lower one-third of the molecular layer (10 psi, 50 msec).

The DISC charge transfer was measured from a 1-sec-long segment centered at the DISC peak. Off-line digital processing of traces was used to high-pass filter the traces at 10 Hz to extract noise information. The noise SD was calculated from a 1-sec-long segment centered at the DISC peak of the digitally high-pass-filtered traces. Δ noise SD was calculated by subtracting the noise SD in a 1-sec-long sample before depolarization (baseline noise SD) from that during the DISC sampling period (Fig. 2h) and normalized by baseline noise SD. Statistical comparisons were performed by using single-factor ANOVA throughout this study.

SR95531 hydrobromide (GABAzine), NBQX, CPCCOEt, JNJ16259685, SKF96365, AIDA, (R)-CPP, nifedipine, and DHPG were purchased from Tocris; Botulinum neurotoxin type D light chain from List Biological Laboratories; bafilomycin A1 from BioMol; ω-agatoxin IVA and ω-conotoxin MVIIC from Alomone Labs; URB597 from Cayman Chemical; Fluo-5F from Invitrogen; and all other chemicals from Sigma. EAAT3/EAAT4 double-knockout mice (17) were gifts from the laboratory of D. Bergles (Johns Hopkins University, Baltimore).

Ca^{2+} Imaging. For Purkinje cell Ca^{2+} imaging, 0.2 mM EGTA in the pipette solution was replaced by 0.3 mM Fluo-5F ($K_d \sim 2.3\ \mu$M), and 0.3 mM Alexa 594 hydrazide (Invitrogen) was added to visualize the soma and dendrite. To minimize phototoxicity, 0.1 mM Trolox-C was added to ACSF, and the power and exposure time of laser illumination were maintained as low as possible. Ca^{2+} transients were elicited by 10-msec-long depolarizing steps from −70 mV to 0 mV, delivered at 1-min intervals, and recorded by a laser-scanning confocal microscope (Zeiss Pascal) with a ×40 water-immersion objective lens. Fluo-5F was excited with the 488-nm line of an Argon ion laser, and emitted fluorescence was collected through a 505-nm long-pass filter. Alexa 594 hydrazide was excited with the 543-nm line of a He-Ne laser, and the fluorescence was collected through a 560 long-pass filter. Fluo-5F images were recorded in frame-scan mode with 128 × 33 pixels at 20 Hz (SI Figs. 5 and 6). For analysis, foreground pixels were determined by thresholding the image and spatially averaged to calculate ΔF/F$_o$ for each frame.

1. Rall W, Shepherd GM, Reese TS, Brightman MW (1966) *Exp Neurol* 14:44–56.
2. Zilberter Y (2000) *J Physiol* 528:489–496.
3. Harkany T, Holmgren C, Hartig W, Qureshi T, Chaudhry FA, Storm-Mathisen J, Dobszay MB, Berghuis P, Schulte G, Sousa KM, *et al.* (2004) *J Neurosci* 24:4978–4988.
4. Duguid IC, Smart TG (2004) *Nat Neurosci* 7:525–533.
5. Duguid IC, Pankratov Y, Moss GW, Smart TG (2007) *J Neurosci* 27:12464–12474.
6. Llano I, Leresche N, Marty A (1991) *Neuron* 6:565–574.
7. Canepari M, Papageorgiou G, Corrie JE, Watkins C, Ogden D (2001) *J Physiol* 533:765–772.
8. Canepari M, Auger C, Ogden D (2004) *J Neurosci* 24:3563–3573.
9. Kim SJ, Kim YS, Yuan JP, Petralia RS, Worley PF, Linden DJ (2003) *Nature* 426:285–291.
10. Tempia F, Miniaci MC, Anchisi D, Strata P (1998) *J Neurophysiol* 80:520–528.
11. Zygmunt PM, Petersson J, Andersson DA, Chuang H, Sorgard M, Di Marzo V, Julius D, Hogestatt ED (1999) *Nature* 400:452–457.
12. Ekerot CF, Oscarsson O, Schouenborg J (1987) *J Physiol* 386:539–546.
13. Gras C, Vinatier J, Amilhon B, Guerci A, Christov C, Ravassard P, Giros B, El Mestikawy S (2005) *Neuropharmacology* 49:901–911.
14. Isaacson JS (1999) *Neuron* 23:377–384.
15. Salin PA, Lledo PM, Vincent JD, Charpak S (2001) *J Neurophysiol* 85:1275–1282.
16. Ludwig M, Leng G (2006) *Nat Rev Neurosci* 7:126–136.
17. Huang YH, Dykes-Hoberg M, Tanaka K, Rothstein JD, Bergles DE (2004) *J Neurosci* 24:103–111.

Shin *et al.*